British Journal of Clinical Pharmacology

DOI:10.1111/bcp.12852

Pharmacokinetic/pharmaco–dynamic modelling and simulation of the effects of different cannabinoid receptor type 1 antagonists on Δ9-tetrahydrocannabinol challenge tests

Zheng Guan, Linda E. Klumpers, Olubukayo-Opeyemi Oyetayo, Jules Heuberger, Joop M. A. van Gerven & Jasper Stevens

Centre for Human Drug Research, Leiden, the Netherlands

Correspondence
Mr Zheng Guan, Zernikedreef 8, 2333 CL, Leiden, The Netherlands.
Tel.: 86 10 5821 8796
Fax: 86 10 5821 4798
E-mail: guanzheng828@gmail.com

Keywords
Δ^9-tetrahydrocannabinol, CB_1 antagonist, modelling and simulation, population pharmacokinetics and pharmacodynamics

Received
4 August 2015

Accepted
25 November 2015

Accepted Article Published Online
30 November 2015

WHAT IS ALREADY KNOWN ABOUT THIS SUBJECT

- Market withdrawal of the cannabinoid receptor type 1 (CB_1) antagonist (rimonabant) negatively affected cannabinoid antagonist research. The recently developed peripheral CB_1 antagonist (e.g. TM38837) showed a larger specificity for peripheral effects than for central effects and confirms potential medical benefit without the central side effects. It is crucial to understand how a specific antagonist affects the central or the peripheral target sites.

WHAT THIS STUDY ADDS

- This study retrospectively collected data of four CB_1 antagonists in THC challenge test in healthy volunteers. Integrated population PK/PD modelling was constructed and benchmark simulations were conducted to compare directly dose–efficacy profiles of different CB_1 antagonists, which gave insight into future development of cannabis based medicines.

AIM

The severe psychiatric side effects of cannabinoid receptor type 1 (CB_1) antagonists hampered their wide development but this might be overcome by careful management of drug development with pharmacokinetic/pharmacodynamic (PK/PD) analyses. PK/PD models suitable for direct comparison of different CB_1 antagonists in Δ^9-tetrahydrocannabinol (THC) challenge tests in healthy volunteer were constructed.

METHODS

The pharmacokinetic models of THC and four CB_1 antagonists were built separately. THC-induced effects on heart rate and the visual analogue scale of feeling high in healthy volunteers and inhibitive effects of CB_1 antagonists on THC-induced effects were modelled in PD models linked to the PK models. Simulations were then applied to evaluate the reduction rate of each antagonist on the reversal of the THC-induced effect in a unified simulation scenario.

RESULTS

The final PK model of THC and antagonists was a two compartment model. An E_{max} model and logistic regression model were used for effect measures and the antagonist effect was added in these models in a competitive binding manner. $t_{1/2ke0}$ ranged from 0.00462 to 63.7 h for heart rate and from 0.964 to 150 h for VAS. IC_{50} ranged from 6.42 to 202 ng ml^{-1} for heart rate and from 12.1 to 376 ng ml^{-1} for VAS. Benchmark simulation showed different dose–efficacy profiles of two efficacy measures for each CB_1 antagonist.

CONCLUSIONS

PK/PD modelling and simulation approach was suitable for describing and predicting heart rate and feeling high for CB_1 antagonists in THC challenge tests. Direct comparison of four antagonists based on simulated efficacy profiles might be of benefit to guide future studies.

Introduction

Obesity is one of the world wide, emerging, serious, life threatening diseases [1]. The lack of efficient and well-tolerated drugs to treat obesity has led to an increased interest in new targets for the development of new drugs [2, 3]. A specifically interesting target is the CB_1 receptor, which is located in the central nervous system (CNS) and at peripheral sites such as the heart, liver, pancreas and adipose tissue [4, 5]. At these sites, the CB_1 receptor has a modulatory role in the regulation of a variety of complex physiological systems, such as the nervous system, and the digestive and endocrine system in metabolism [for a review, see [6]]. Activation of the CB_1 receptor leads to effects including feeling high and altered time perception, increased body sway and getting hungry ('the munchies') (for a review, see [7]).

This widespread involvement of the CB_1 receptor and its ligands provides numerous opportunities for the development of new medicines for neuronal and metabolic disorders including movement disorders, diabetes mellitus and dyslipidaemia. In the late 1990s the pharmaceutical industry became particularly interested in the metabolism effects of CB_1 receptors and focused on new chemical entities that could decrease appetite by CB_1 receptor antagonism. It was found that CB_1 antagonists were indeed able to block feeding behaviour and they also showed other characteristics (including decreased gastric emptying and increased insulin sensitivity [2, 8]) that underlined the potential of CB_1 antagonists in obesity treatment.

In 2006, the first CB_1 antagonist rimonabant (formerly known as SR141716) was registered for the treatment of obesity and overweight with obesity-associated disorders [9]. Besides rimonabant, Sanofi developed more CB_1 antagonists, such as drinabant (formerly known as AVE1625 with possible inverse agonism properties) and surinabant (SR147778). However, in 2008, rimonabant was withdrawn from the market due to unacceptable psychiatric adverse effects. Almost all pharmaceutical companies, including Sanofi, terminated all studies involving CB_1 receptor antagonists (such as rimonabant, otenabant and taranabant).

Nevertheless, there are studies suggesting that the beneficial metabolic effects of rimonabant might be regulated predominantly by peripheral CB_1 receptors, whereas the psychiatric side effects could be regulated by centrally located CB_1 receptors [10, 11]. There is considerable evidence to suggest that the beneficial metabolic effects of CB_1 antagonists are mediated by CB_1 receptors that are present at locations which are specifically associated with metabolic regulation, such as the liver, the pancreas and fat cells [4, 5, 12]. If the therapeutic effects of CB_1 antagonists have their target site in peripheral tissues and the (serious) side effects originate in certain regions of the CNS, it is crucial to understand how a specific antagonist could affect the several central and the peripheral target sites.

One of the problems with the investigation of the different sites and effects of CB_1 antagonism is that there are no validated measurements of these effects after acute administration of CB_1 antagonists or in healthy subjects. To partly overcome this problem, challenge tests with the $CB_{1/2}$ partial antagonist Δ^9-tetrahydrocannabinol (THC) were developed [13–15]. With this challenge test, the endocannabinoid system is stimulated using THC, which induces a range of dose- and concentration-related responses. Several of these measures, such as the characteristic euphoric 'high' feeling, are clearly indicative of central nervous system effects. Other parameters like heart rate are more likely to be peripherally mediated [14, 16]. The THC challenge has been found to be an effective tool to demonstrate the pharmacological effects of a CB_1 antagonist, since co-administration of a selective CB_1 antagonist causes a near complete block of the acute THC-induced effects. The use of the variety of measures such as feeling high, body sway and heart rate allow us to create individual effect profiles for the different CB_1 antagonists.

Previously, our clinical research centre separately investigated the concentration–effect relationships of four different CB_1 antagonists, rimonabant, surinabant, AVE1625 (drinabant) and TM38837 [13, 17]. This was performed in three separate studies by using THC challenge tests, all with different THC dosages and dosing time intervals. This approach allowed us to analyze the pharmacological characterization of the individual antagonists. However, a thorough comparison among the antagonists was hampered by the different dose regimes of the THC challenge tests. In the current study, we built an integrated pharmacokinetic/pharmacodynamic (PK/PD) model for all antagonists that would compensate for these differences between the THC challenge tests,

allowing a direct comparison of the different CB_1 antagonists with regards to PK and PD characteristics.

PK/PD modelling is an approach to characterize the concentration–time profile and the relationship between concentrations and effects using a mathematical model. Model estimation can be based on both individuals and populations. The assumption that all individual concentration–effect relationships can be described with the same structural model is based on the notion that the drug activates the same pharmacological system in all subjects (or systems for different responses). PK/PD modelling is performed by using a non-linear mixed effect modelling approach which provides estimates of the population average parameters (assuming that each individual can be described using the same structural model) and their associated inter-individual variability, which allows individuals to differ from each other. Residual error describing the variability of the difference between predicted values and the observations is also estimated [18, 19]. Simulation is a subsequent step, following the modelling. It can be used to predict model outcomes using an existing model structure given different scenarios (model input), for instance with different dosages, sampling times and other covariates.

Our first aim was to build an integrated PK/PD model that would be suitable for direct comparisons of pharmacological compounds in a complex clinical setting using a pharmacological challenge test. We would do this for four different CB_1 antagonists (drinabant, surinabant, rimonabant and TM38837) and a THC challenge test for efficacy parameters feeling high and heart rate. Our second aim was to apply the model for direct comparisons of the different pharmacokinetic profiles and efficacy of the four different CB_1 antagonists to understand better the behaviour of CB_1 antagonists in healthy humans.

Methods

Study designs

From 2003 until 2009, three THC challenge studies were performed at CHDR in healthy male volunteers, in which four CB_1 antagonists were administered, a study with drinabant (AVE1625), one with surinabant (SR147778) and another study that investigated both rimonabant (SR141716) and TM38837 (referred to as 'the rimonabant-TM38837 study') [16, 20]. The three studies were all performed in a double-blind, randomized, placebo-controlled, (partial) crossover manner. The complete design and clinical results of these studies were published separately [13, 17]. The treatments per study and subject demographics are summarized in Table 1 and Table 2, respectively. In short, each CB_1 antagonist or placebo administration was followed by a series of inhaled doses of a vaporized solution of THC in ethanol or THC vehicle, which consisted only of vaporized ethanol. THC was vaporized using a Volcano vaporizer® (Storz & Bickel GmbH & Co. KG, Tuttlingen, Germany). In each study, the first THC dose was administered around the expected t_{max} of the CB_1 antagonist. Blood samples for PK and selected PD responses were taken accordingly after multiple THC challenge and/or antagonist administration and the last sampling time points were shortly after the last challenge dose of THC.

Table 1

Subject demographics. Mean with standard deviation (SD)

Name of study	Subject number	Age (years)	Weight (kg)	Height (cm)	BMI (kg m^{-2})
Drinabant	36	22.0 (3.0)	76.0 (11.0)	183.0 (6.0)	23.0 (3.0)
Surinabant	30	23.2 (5.3)	79.0 (8.2)	187.7 (6.7)	22.4 (1.9)
Rimonabant-TM38837	36	21.2 (3.8)	77.3 (10.2)	183.4 (7.0)	22.9 (2.1)

BMI, body mass index.

Pharmacokinetic and pharmacodynamic measurements

Blood samples of THC and four antagonists were analyzed as published before [13, 17]. In short, THC samples were measured using tandem mass spectrometry with a lower limit of quantification of 0.1 ng ml^{-1}. Concentration of AVE1625 was measured using flow chromatography-mass spectrometry/mass spectrometry (TFC-MS/MS) and the limit of quantification was 0.2 ng ml^{-1}. The concentration of surinabant was measured using liquid chromatography coupled with a tandem mass spectrometry (LCMS/MS) method with a lower limit of quantification (LLOQ) of 1.0 ng ml^{-1}. Concentrations of TM38837 and rimonabant were measured by liquid chromatography with a tandem mass spectrometry method with a lower limit of quantification of 0.1 ng ml^{-1} for TM38837 and 1.0 ng ml^{-1} for rimonabant.

In all studies, visual analogue scales (VAS) according to Bowdle (psychedelic effects) and heart rate were assessed frequently [15, 21]. Heart rate was measured using a Nihon-Koden BSM-1101 K monitor (Lifescope EC, Tokyo, Japan) blood pressure apparatus. The adapted version of the Bowdle scales consists of 100 mm visual analogue lines, to indicate subjective feeling high, and on a range of other subjective effects that cluster as factors internal perception and external perception, both composite scores that are affected differently by THC as previously described [15].

Modelling and simulation

PK and PK/PD modelling was performed using a population approach non-linear mixed effect modelling program, NONMEM 7.1.0 [18]. Non-linear mixed effect modelling considers the repeated observations as a function of time in a population of individuals. The model to describe these observations adopts a common structural model and distribution of residuals, while allowing the

Table 2

Treatments per study

Name of study	Treatment	Time of THC administration after antagonist administration (h)	THC challenge administration dosage (mg)
Drinabant	Placebo drinabant + THC vehicle	3, 4, 5, 6	2, 4, 6, 6
	Placebo drinabant + THC challenge		
	20 mg drinabant + THC challenge		
	60 mg drinabant + THC challenge		
	120 mg drinabant + THC challenge		
	120 mg drinabant + THC vehicle		
Surinabant	Placebo surinabant + THC vehicle	1.5, 2.5, 3.5, 4.5	2, 4, 6, 6
	Placebo surinabant + THC challenge		
	5 mg surinabant + THC challenge		
	20 mg surinabant + THC challenge		
	60 mg surinabant + THC challenge		
	60 mg surinabant + THC vehicle		
Rimonabant-TM38837	Placebo TM38837 + Placebo rimonabant + THC vehicle	2, 4.5, 7, 22, 24.5*	4, 4, 4, 4, 4
	Placebo TM38837 + Placebo rimonabant + THC challenge		
	100 mg TM38837 + Placebo rimonabant + THC challenge		
	500 mg TM38837 + Placebo rimonabant + THC challenge	4, 6.5, 9, 24, 26.5†	4, 4, 4, 4, 4
	Placebo TM38837 + 60 mg rimonabant + THC challenge		
	Placebo TM38837 + Placebo rimonabant + THC challenge		

*Time of THC administration after rimonabant administration. †Time of THC administration after TM38837 administration.

parameters in the model to vary between individuals. The location (typical value or fixed effect) and spread between individuals (variability or random effect) of the model parameters are estimated by fitting the parameters to the data by minimizing an objective function based on the log likelihood ($-2 \times$ LL). Using the population values (both location and spread), individual specific empirical Bayes' estimates (*post hoc* estimates of individual deviates (ETAs) from the random effects distributions) are determined that allow description of individual time profiles.

Different models are compared with increasing complexity in the structural model and the number of random effects. The objective is to find the simplest model that describes the data adequately. Competing models are compared using the likelihood ratio test, which compares the difference between log-likelihoods for the models (difference in objective function value, ΔOFV) to a chi-square distribution with degrees of freedom corresponding to the difference in number of parameters between the two models (P value used was less than 0.01: ΔOFV = -6.63). Models were qualified by visual inspection for goodness of fit and check of weighted residuals.

A general overview of the two step modelling approach is displayed in Figure 1. First, PK models for THC and the four antagonists were built separately for every compound to obtain estimated PK parameters based on OFV and goodness of fit. The PK model was only built to describe optimally the PK profile. Therefore, a separate THC model (if possible with a similar structure) was built for each of the three studies. Secondly, the PK/PD model was built. The integrated models only regard the PD models to enable direct comparison of the different CB_1 antagonists. Individual empirical Bayes' estimates were determined to describe the concentration profile and used in the subsequent PK/PD analyses. Parameter estimation for population PK modelling of THC and antagonists was performed under ADVAN 5 and the PK/PD

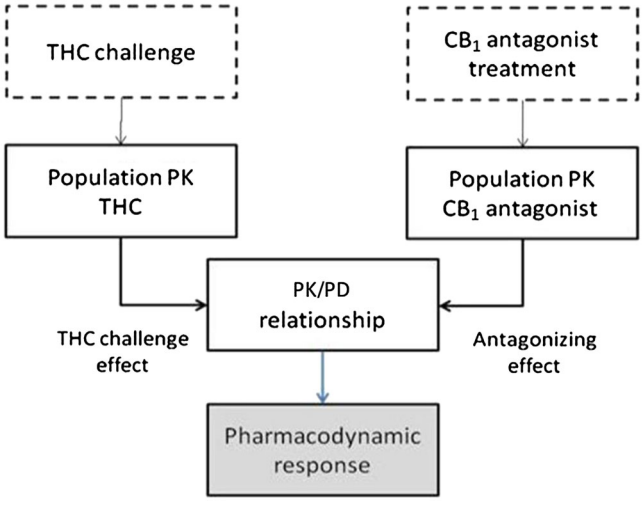

Figure 1

Schematic representation of the PK/PD models

modelling of all PD parameters was performed under ADVAN6 TOL 5. The RSE (relative standard error) was calculated for all parameters. Inter-individual variability (IIV) and inter-occasion variability was expressed as coefficient of variation (%CV) using:

$$\%CV = 100 \times \sqrt{\exp(\omega^2) - 1} \quad (1)$$

First order conditional estimation (FOCEI) with interaction was the standard method of estimation, with the exception of VAS feeling high PD model, for which LAPLACE was used. Within each model, additive and/or proportional residual error models were compared.

Pharmacokinetic and pharmacodynamic analyses

The population PK model of THC was based on the results of previous CHDR studies with multiple THC inhalations, using a two compartment model with bolus administration [14] and first order elimination. PK analyses of the four antagonists were performed in a similar way with compartmental model, including first order absorption and first order elimination.

A biophase compartment is used when drug action is delayed by distribution from plasma to the site of action. The rate of equilibration of drug in the plasma with the site of action is denoted k_{e0}, the rate constant for exit of drug from the biophase compartment [22–24].

A biophase compartment was first used to account for the delayed response of VAS. To minimize the effect of over- and under-dispersion due to the subjectivity of the VAS scale and to include non-response in the model, the VAS feeling high scale was translated into a binary scale, to accommodate the possibility to construct a probability model for feeling high. The anchor point for this translation was the median of all scores higher than 0 (on a 100 point scale) for the treatment arms where only THC was dosed. Inverse logit transformation is used for binary data:

$$P(VAS > CUT) = \frac{\exp(-k_d \times TAD) \times \exp(x)}{1 + \exp(x)} \quad (2)$$

with

$$x = \frac{\beta_1 \cdot C_{THC}}{1 + \beta \cdot C_{Antgonist}} \quad (3)$$

in which CUT was the anchor point that changed depending on the study, β_1 is the coefficient of THC effect and $\beta$is the coefficient of the shift of the THC effect caused by the antagonist. The effect of antagonists in the above equation reverses the THC induced increase in probability of scoring a VAS > CUT. Every subject receives multiple THC inhalations, causing a tolerability that affected the scores of the VAS. To cope with this, K_d, the elimination rate of tolerance, was included to decrease the possibility of feeling high caused by time factor TAD, the time after the first dosing time point.

A biophase compartment was used to account for the delayed response of heart rate as well. Because all the antagonists bind with the CB_1 receptor in competition with THC, the biophase compartment concentration of THC and respective antagonist was used for the PD analyses by using a maximum effect equation (Equation (4)). In this equation, the antagonist could cause a shift to the right of the apparent EC_{50} depending on the impact of the THC challenge effect and the effect is described as:

$$E = E_0 + \frac{E_{max} \times C_{THC}}{EC_{50} + C_{THC} + \beta \times C_{Antagonist}} \quad (4)$$

where E_0 is the baseline of the effect, E_{max} is the maximal achievable effect, C_{THC} is THC concentration in biophase compartment, EC_{50} is the concentration that causes 50% of the E_{max}, β is the coefficient that describes the antagonist shift by the THC effect and $C_{Antagonist}$ is the CB_1 antagonist concentration in the biophase compartment. In practice, it was observed that the baseline of heart rate was around 60 beats min^{-1}. After treatment with THC or together with CB_1 antagonists, heart rate increased. Once heart rate became higher than around twice that of the baseline, there was a big proportion of the subjects who could not finish the rest of the measurements. Given this observation, we tried two approaches which were fixing E_{max} effect to two folds of baseline or estimating E_{max} without fixing it.

Based on PD model parameters, IC_{50} and $t_{1/2ke0}$ can be then be derived from parameter estimation by using equations (3) and (4). These two parameters describe the inhibition potential of CB_1 antagonists. IC_{50} is a measure of the effectiveness of a compound in inhibiting biological function. It indicates how much of a particular antagonist is needed to inhibit a given effect of THC by half. $t_{1/2e0}$ is the apparent half-life of a drug effect. It is derived from k_{e0}, which indicates the rate constant of the elimination of a drug effect:

$$IC_{50} = \frac{EC_{50}}{\beta} \quad (5)$$

$$t_{1/2ke0} = \frac{\log 2}{k_{e0}} \quad (6)$$

Visual predictive checks

Visual predictive checks (VPC) were performed for all PK and PD models using R version 2.12.0 (R: A Language and Environment for Statistical Computing, R Development Core Team, R Foundation for Statistical Computing,

Vienna, Austria, 2010) with the lsoda (deSolve Package 1.8.1) and mvrnorm functions (MASS Package v7.3–8). The visual predictive check encompassed a projection of the simulated dependent variable as a function of time using the final model on the observations. The simulations were performed considering the estimated population parameters (Θ vector) as well as the covariance matrix describing IIV (Ω matrix). The residual variability (Σ matrix) was not included in the simulations. The simulations and the data were grouped by dose of antagonists. Summary statistics of the simulations (median and the 95% prediction interval of the simulated IIV) enabled a comparison of the predicted and the observed variability. For each dose group 1000 individuals were simulated.

Simulation

We selected a benchmark scenario to try to cover maximally the major part of the original study designs. Due to differences in t_{max}, the time points of the first THC administration relative to the antagonist administration were different among the different study designs. As original study designs, the time between administration of CB_1 antagonists and first THC was the same as the t_{max} of antagonist. In this way, the first THC inhalation would be administered at the expected t_{max} of CB_1 antagonists. We kept this the same in the benchmark scenario and we compensated for these differences by simulating the THC challenge profile rather than using the actual challenges. During this simulated challenge, individuals received four doses (2, 4, 6 and 6 mg) of THC inhalation at hourly intervals. Drinabant, surinabant, rimonabant and TM38837 were simulated as single dose administered at 3, 1.5, 2 and 4 h before THC challenge, respectively, similar to the dose regimens in the actual studies. A wide dose range of the antagonists was simulated with dosages from 2 mg to 1000 mg to optimize the dose–response curve. For surinabant, when dose is higher than 60 mg, the simulation used a surinabant PK model with the assumption that K_a did not change when dose was higher than 60 mg. The reduction ratio (RR) was used as drug response in the dose–response curve and was calculated as the difference between the area under the curve (AUC) of the PD response of the THC challenge only and the THC challenge + antagonist. For AUC calculation observations were used from the first administration of THC until 1 h after the fourth THC administration. The reduction rate was calculated as:

$$RR = \frac{AUC_{THC} - AUC_{Antagonist+THC}}{AUC_{THC}} * 100 \quad (7)$$

where RR is the reduction ratio, AUC_{THC} is the area under the curve of THC alone and $AUC_{Antagonist\ +\ THC}$ is the area under the curve of co-administration of THC and the antagonist. The difference between RRs of two PD markers for each drug will also be calculated to assist effects comparison and dosage selection.

Simulations were performed in a similar way as for VPC by implementing the identified models and the estimated parameters in R using the function lsoda from the deSolve library (version 1.8.1) and the function mvrnorm from the MASS library (version 7.3–8). The results of the simulations were used to plot the population typical dose–response curves.

Results

THC pharmacokinetic modelling

In all three studies, a two compartmental structure model with first order elimination was the best model to describe the THC concentration–time curve. The pulmonary administration was implemented as a bolus input in the central compartment.

The PK parameters of THC of the three separate studies are presented in Table 3. No significant differences were found among the studies for the model parameter estimations and they were also similar to the parameters from the models by Strougo *et al.* [14]. All RSEs of the estimations were smaller than 30% (from 5.2% to 14.3%). Inter-individual variability (IIV) was identified on the apparent central distribution volume, ranging from 10.3% to 40.8%. IIV on apparent clearance was 18.8% and 31.2% for the drinabant study and the rimonabant-

Table 3

PK parameters of THC in the different studies, with the relative standard error (RSE, %) and the inter-individual variability (IIV) as %CV

	Drinabant			Surinabant			Rimonabant-TM38837		
Parameter	Estimate (%RSE)	IIV	IOV	Estimate (%RSE)	IIV	IOV	Estimate (%RSE)	IIV	IOV
Clearance/*F* (l h^{-1})	228.1 (5.2)	18.8	-	228.1 (7.4)	-	-	200 (5.9)	31.2	-
Central volume/*F* (l)	35.5 (7.0)	10.3	-	35.2 (8.9)	38.5	76.0	28.5 (8.9)	40.8	25.1
Peripheral volume of distribution/*F* (l)	145.4 (6.5)	-	-	103.4 (6.8)	-	-	107 (14.3)	-	-
Intercompartmental clearance/*F* (l h^{-1})	134.3 (6.1)	-	-	127.7 (7.2)	-	-	106 (6.9)	-	-

F, bioavailability; IOV, inter-occasion variability (%).

TM38837 study, separately. For the surinabant study the IIV on the apparent clearance could not be identified. Additionally, inter-occasion variability on the apparent central distribution volume was included to account for differences in bioavailability between individual dosing occasions in the surinabant study and the rimonabant-TM38837 study and was 78.0% and 25.1%, respectively. The residual error model was only proportional to concentration.

Antagonist pharmacokinetic modelling

The PK models of the four antagonists were built separately. All of them could be described using a two compartmental model with first-order elimination and first order absorption. Surinabant was found to have a lag time of 0.6 h (RSE = 5.7%) and its k_a was dose-proportional with a dose effect of 0.005 (RSE = 14.4%) as defined by the following equation:

$$k_a(\text{dose}) = 0.4 \times (1 - \alpha \times \text{dose}) \quad (8)$$

in which α is the dose effect to k_a. For each compound, the RSEs of the parameter estimations varied between 3.9% and 42.4% (Table 4). IIV and IOV were incorporated in the model if it improved goodness of fit. IIV for the clearance of surinabant, rimonabant and TM38837 ranged from 25.6% to 66.2%. For apparent central distribution volume, the IIV varied from 20.6% to 132.0%. The goodness of fit plot was improved by adding an IOV of 24.0% for the central distribution volume of drinabant. Inspection of the data showed that the upswing of the concentration after administration of rimonabant was insufficiently detailed to estimate the first order absorption rate constant. Therefore, this parameter was fixed to the value for the absorption rate constant as reported by Martinez [25]. The PK parameter estimations of the antagonists were presented separately in Table 4, including the RSE, inter-individual variability and inter-occasion variability. VPCs and diagnostic plots were also performed for all four antagonists PK model for model validation.

Table 5

PK/PD parameter estimates of THC alone for heart rate and VAS feeling high with percentage coefficient of variation (CV)

	Parameter	Units	Estimate (%RSE)	IIV	IOV
Heart rate	$t_{1/2}$	(h)	0.3. (28.2)	--	--
	E_0	(beats min^{-1})	64.2 (1.1)	8.0	5.9
	E_{max}	(beats min^{-1})	64.2 (––)	--	--
	EC_{50}	(ng ml^{-1})	73.7 (18.4)	--	--
Feeling high	$t_{1/2}$	(h)	2.3 (16.3)	--	--
	CUT1		2.8 (3.0)	--	--
	βTHC		−0.5 (16.7)	--	--
	K_d		0.1 (18.6)	--	--

t_{50}, equilibration half-life of the elimination from the biophase compartment; E_{max}, maximal effect; EC_{50}, concentration at 50% of maximal effect; IIV, inter individual variability; IOV, inter occasion variability; βTHC, coefficient of the antagonist-induced shift of the THC effect; K_d, elimination rate of tolerance.

The THC-induced effects were modelled using data from treatment arms with THC dosages only. To enable a direct comparison of the antagonists, an integrated THC PD model was applied on the three trials for the same set of PD parameters, heart rate and feeling high. An E_{max} model gave the best fit for heart rate. The baseline was estimated at 64.2 beats min^{-1} with a RSE of 1.1%. Within the study, the highest heart rate observed was around 120 beats min^{-1}. Although physiologically, higher heart rates are possible for higher THC dosages, we chose to fix the E_{max} of heart rate to two times the baseline, resulting in proper diagnostic plots and VPCs. IIV and IOV were both incorporated at the baseline at 7.98% and 5.91%. RSEs of all heart rate model parameters were below 30%.

A logistic regression model was used for modelling the VAS feeling high, the parameters of which had a relatively low RSE (smaller than 20%). The estimated parameters of VAS feeling high are shown in Table 5.

Antagonist pharmacodynamic modelling

An effect compartment was built for THC and the antagonists to describe the time delay between the

Table 4

PK parameters of drinabant, surinabant, rimonabant and TM38837 with the relative standard error (RSE, %) and the inter-individual variability (IIV) as %CV

	Drinabant			Surinabant			Rimonabant			TM38837		
Parameter	Estimate (%RSE)	IIV	IOV	Estimate (%RSE)	IIV	IOV	Estimate (%RSE)	IIV	IOV	Estimate (%RSE)	IIV	IOV
Clearance/*F* ($l\ h^{-1}$)	32.5(14.8)	-	-	4.4(12.7)	62.5	-	9.3 (6.9)	25.6	-	2.2 (9.3)	66.2	-
Central volume/*F* (l)	212.7(9.6)	36.3	24.0	5.0(16.3)	66.4	-	39.3 (15.5)	20.6	-	18.7 (16.3)	132.0	-
Peripheral volume of distribution/*F* (l)	2164.6(30.0)	-	-	515.0(12.5)	102.0	-	93.0 (12.8)	-	-	10.8 (42.4)	-	-
Intercompartmental clearance/*F* ($l\ h^{-1}$)	32.5(11.4)	-	-	15.9(6.5)	91.2	-	17.9 (17.2)	-	-	0.01 (22.0)	-	-
Absorption rate constant (k_a, h^{-1})	1.1(8.2)	39.8	-	0.4(3.9)	7.8	-	1.2 (fixed)	-	-	0.08(9.7)	-	-
Dose effect on k_a* (α)	-	-	-	0.005(14.4)	-	-	-	-	-	-	-	-
Lag time(h)	-	-	-	0.6 (5.7)	-	-	-	-	-	-	-	-

Dose effect on k_a: k_a (dose) = $k_a \times (1 - \alpha \times \text{dose})$. [1]*F*, bioavailability; IOV, inter-occasion variability (%).

concentration–effect profiles. For the heart rate model, fixing approach showed better model fitting and prediction on both a population and individual level given one less parameters estimate. Therefore, fixing approach was selected for the final heart rate model. An equilibration half-life ($t_{1/2keo}$) was defined, which ranged from 0.005 (0.5%) to 63.7 (35.4%) h for heart rate with all RSEs smaller than 100% and 1.0 (193.0%) to 150.0 (16.8%) h for VAS. These wide CV ranges suggested a large variability in drug distribution rates to the target locations for the different antagonists. Rimonabant presented a relatively high RSE, which was the only one that was bigger than 100%. This suggested a low uncertainty of the parameter estimation.

The range of IC_{50} also varied widely, from 6.4 (36.9%) to 202.0 (38.6%) ng ml^{-1} for heart rate and from 12.1 (25.9%) to 376.0 (15.3%) ng ml^{-1} for VAS feeling high with all RSE smaller than 100%.

All PD parameter estimates of the four different antagonists are presented in Table 6. Both diagnostic plot and VPC were performed, which confirmed that the proposed model fitted the data properly with acceptable predictive ability.

Table 6

PK–PD parameter estimates of antagonists for VAS feeling high, body sway and heart rate with percentage coefficient of variation (CV)

	Parameter	Units	Estimate(%RSE)	Estimate(%RSE)	Estimate(%RSE)	Estimate(%RSE)
			Drinabant	Surinabant	TM38837	Rimonabant
Heart rate	$t_{1/2e0}$	(h)	6.3(34.6)	0.005(0.5)	63.7(35.4)	1.1(26.3)
	IC_{50}	(ng ml^{-1})	6.4(36.9)	107.0(34.4)	175.0(36.6)	202.0(38.6)
Feeling high	$t_{1/2e0}$	(h)	1.8(34.7)	6.7(62.9)	150.0(16.8)	1.0(193.0)
	IC_{50}	(ng ml^{-1})	12.1(25.9)	61.6 (44.9)	376.0(15.3)	92.8(65.0)

$t_{1/2e0}$, equilibration half-life; IC_{50}, concentration of antagonist at 50% of maximal inhibition.

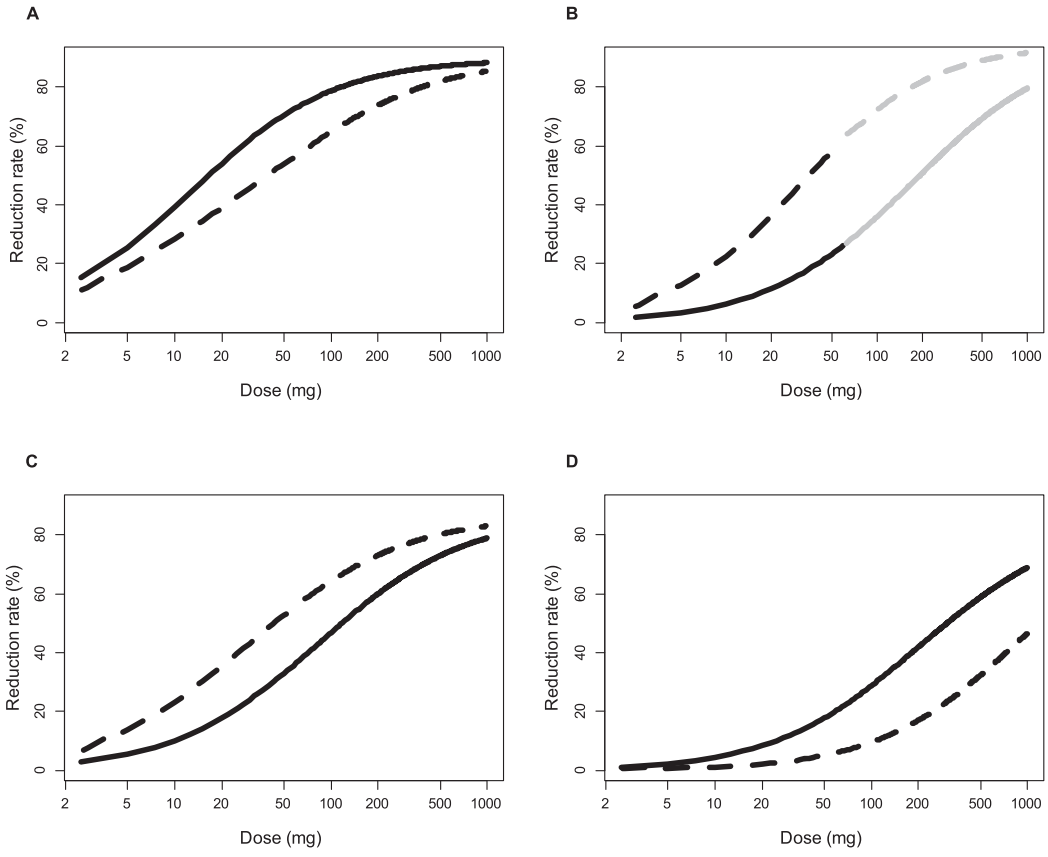

Figure 2

Simulated dose–effect relationship and the estimated reduction rate (i.e. antagonism of THC-induced effects) of heart rate (solid line) and VAS feeling high (dashed line) of (A) drinabant, (B) surinabant, (C) rimonabant and (D) TM38837. The grey line represents that for surinabant, when dose is higher than 60 mg, the simulation used surinabant PK model with assumption that K_a did not change when dose was higher than 60 mg

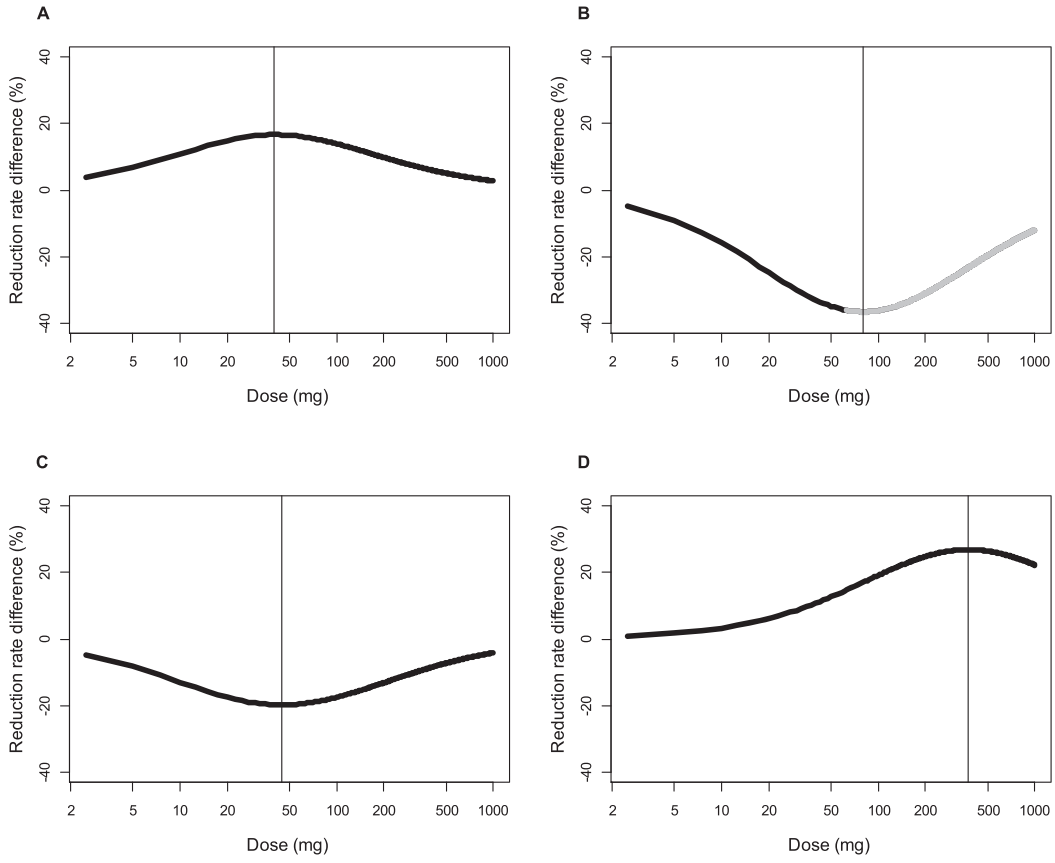

Figure 3

Simulated dose-estimated reduction rate difference of heart rate and feeling high: (A) drinabant; (B) surinabant; (C) rimonabant; (D) TM38837. The grey line represents that for surinabant, when dose is higher than 60mg, the simulation used surinabant PK model with assumption that Ka did not change when dose was higher than 60mg

Dose–response curve simulations

The simulations of two dose–response curves (in this case dose reduction rate curves) of the antagonists are graphically displayed in Figure 2. The dose range for the simulation ranged from 2 to 1000 mg. All antagonists caused a maximal reduction of THC-induced effects of 70% to 85%. The order and shape of the curves that depict the relations between dosages and reduction rates varied considerably among the different CB_1 antagonists and effects. For example, the reduction rates for heart rate were larger than for VAS feeling high in the case of drinabant and TM38837, whereas for surinabant and rimonabant, VAS feeling high had a higher reduction rate than heart rate. A set of plots derived from Figure 2 which calculated the difference between heart rate RR and VAS feeling high RR changed via dose increasing were also generated as shown in Figure 3. Positive reduction rate difference represented higher effect on heart rate while negative reduction rate difference represented higher effect on VAS feeling high. The plot also provided the maximum and minimum reduction rate difference which could provide a dosage selection indicator to find out the preferred dosage. For example, drinabant and TM38837 showed constant positive reduction difference. This indicated that these two CB_1 antagonists showed better effects on heart rate and the maximum value of the lines suggested that they presented the biggest difference between heart rate and VAS feeling high effect at doses around 40 mg and 380 mg, separately. For surinabant and rimonabant, they consistently showed a bigger effect on VAS feeling high and the maximum difference of the two PD markers was achieved at a dosage of 80 mg and 45 mg separately.

Discussion

Our aims were to build integrated PK/PD models for THC and four CB_1 antagonists and to apply them for direct comparison of the different antagonists to improve our understanding of the behaviour of CB_1 antagonists in healthy volunteers.

We found that our PK/PD modelling and simulation approach was suitable for direct comparisons of pharmacological compounds in complex clinical settings using a THC challenge test, even when the data

camefrom different studies with different THC dosing regimens. Our integrated PK/PD models have a few advantages and disadvantages compared with the individual PK/PD models that we built in previous studies [13, 14, 17]. Integration on the PD level enabled us to compare the different antagonists directly. However this approach resulted in enlarged inaccuracy of parameter estimation. The method of calculating the inhibition ratios of the antagonists as performed in the surinabant study and the rimonabant-TM38837 study was highly dependent on sampling time points and did not consider the whole effect–time profile [13, 14, 17], while our study presented an improved method to calculate inhibition ratios based on the AUC of PD responses. In this way, we were able to make estimations along the whole time–effect curve.

We have found that surinabant and rimonabant induced larger effects on inhibition of THC-induced VAS feeling high than on inhibition of THC-induced heart rate increase, whereas drinabant and TM38837 showed an opposing behaviour. This was consistent when (graphically) comparing the findings from previous studies [13, 15, 17]. The different effect profiles in healthy humans of drinabant and TM38837 compared with surinabant and rimonabant suggest differences in clinical efficacy in patient groups. Considering the previously suggested associations of heart rate effects and peripheral effectivity, it would be tempting to imply that drinabant and TM38837 have a larger preference for peripheral target sites, resulting in larger peripheral effects compared with centrally induced effects. This would be a more desired effect profile, considering the severe unwanted psychiatric side effects as previously observed at clinical rimonabant dosages. However, patient studies are needed to investigate the efficacy of compounds with increased peripheral selectivity and their translation to efficacy parameters in healthy volunteers.

Despite the market withdrawal of rimonabant, it would still be very interesting to investigate the efficacy and tolerability of rimonabant as well as surinabant in more detail. From our previous research [17], we analyzed that the clinically used CB_1 antagonist dosages and steady-state plasma concentrations were well above the dosage and concentration that maximally blocked THC-induced effects. The analyses were performed over specific time periods during which the antagonist concentrations where at maximum reaching maximum inhibition of THC-induced effects. This implies that the clinically applied rimonabant dosage might have been higher than needed to induce favourable therapeutic effects and high enough to induce severe unwanted side effects. We hypothesize that a lower dose and concentration of rimonabant (and the right dose for surinabant) might result in an acceptable balance between efficacy and side effects, which could be different for different patient groups. To confirm this, future research should perform additional patient studies and carefully translate our model (i.e. the results from studies in healthy subjects) to patient groups.

In conclusion, we were able to build suitable PK/PD models in which the CB_1 antagonists, drinabant, surinabant, rimonabant and TM38837, and the agonist THC were integrated. We found that the effects of the antagonists showed different profiles, with drinabant and TM38837 showing relatively larger heart rate effects than effects on VAS feeling high compared with surinabant and rimonabant. The graphic result (Figure 3) also helped dose selection. We suggest that drinabant and TM38837 might have a larger therapeutic potential than rimonabant and surinabant, due to the potential higher risk of severe psychiatric side effects for the latter two compounds, which is based on their relatively large central effects (i.e. feeling high).

Competing Interests

All authors have completed the Unified Competing Interest form at http://www.icmje.org/coi_disclosure.pdf (available on request from the corresponding author) and declare no support from any organization for the submitted work, no financial relationships with any organizations that might have an interest in the submitted work in the previous 3 years and no other relationships or activities that could appear to have influenced the submitted work.

REFERENCES

1 Obesity and overweight - Fact sheet. Available at http://www.who.int/mediacentre/factsheets/fs311/en/index.html (last accessed January 2015)

2 Patel PN, Pathak R. Rimonabant: a novel selective cannabinoid-1 receptor antagonist for treatment of obesity. Am J Health Syst Pharm 2007; 64: 481–9.

3 Barth F. CB_1 cannabinoid receptor antagonists, Annu Rep Med Chem 2005; 40: 103–18.

4 Bermudez-Silva FJ, Suarez J, Baixeras E, Cobo N, Bautista D, Cuesta-Munoz AL, Fuentes E, Juan-Pico P, Castro MJ, Milman G, Nadal A, Rodríguez de Fonseca F. Presence of functional cannabinoid receptors in human endocrine pancreas. Diabetologia 2008; 51: 476–87.

5 Bermudez-Silva FJ, Viveros MP, McPartland JM, Rodriguez de FF. The endocannabinoid system, eating behavior and energy homeostasis: the end or a new beginning? Pharmacol Biochem Behav 2010; 95: 375–82.

6 Melamede R. Harm reduction-the cannabis paradox, Harm Reduction Journal 2005; 2 (Article 17). DOI: 10.1186/1477-7517-2-17.

7 Zuurman L, Ippel AE, Moin E, van Gerven JM. Biomarkers for the effects of cannabis and THC in healthy volunteers. Br J Clin Pharmacol 2009; 67: 5–21.

8 Xie S, Furjanic MA, Ferrara JJ, McAndrew NR, Ardino EL, Ngondara A, Bernstein Y, Thomas KJ, Kim E, Walker JM, Nagar S, Ward SJ, Raffa RB. The endocannabinoid system and rimonabant: a new drug with a novel mechanism of action involving cannabinoid CB_1 receptor antagonism--or inverse agonism--as potential obesity treatment and other therapeutic use. J Clin Pharm Ther 2007; 32: 209–31.

9 Wathion N. Public statement on Acomplia (rimonabant): Withdrawal of the marketing authorisation in the European Union. In Book Public statement on Acomplia (rimonabant): Withdrawal of the marketing authorisation in the European Union, European Medicines Agency, 2009.

10 Cluny NL, Vemuri VK, Chambers AP, Limebeer CL, Bedard H, Wood JT, Lutz B, Zimmer A, Parker LA, Makriyannis A, Sharkey KA. A novel peripherally restricted cannabinoid receptor antagonist, AM6545, reduces food intake and body weight, but does not cause malaise, in rodents. Br J Pharmacol 2010; 161: 629–42.

11 Nogueiras R, Veyrat-Durebex C, Suchanek PM, Klein M, Tschop J, Caldwell C, Woods SC, Wittmann G, Watanabe M, Liposits Z, Fekete C, Reizes O, Rohner-Jeanrenaud F, Tschöp MH. Peripheral, but not central, CB_1 antagonism provides food intake-independent metabolic benefits in diet-induced obese rats. Diabetes 2008; 57: 2977–91.

12 Gomez R, Navarro M, Ferrer B, Trigo JM, Bilbao A, Del Al, Cippitelli A, Nava F, Piomelli D, de Rodriguez FF. A peripheral mechanism for CB_1 cannabinoid receptor-dependent modulation of feeding. J Neurosci 2002; 22: 9612–7.

13 Klumpers LE, Roy C, Ferron G, Turpault S, Poitiers F, Pinquier J-L, van Hasselt JG, Zuurman L, Erwich FA, van Gerven JM. Surinabant, a selective cannabinoid receptor type 1 antagonist, inhibits delta9-tetrahydrocannabinol-induced central nervous system and heart rate effects in humans. Br J Clin Pharmacol 2013; 76: 65–77.

14 Strougo A, Zuurman L, Roy C, Pinquier JL, van Gerven JM, Cohen AF, Schoemaker RC. Modelling of the concentration--effect relationship of THC on central nervous system parameters and heart rate - insight into its mechanisms of action and a tool for clinical research and development of cannabinoids. J Psychopharmacol 2008; 22: 717–26.

15 Zuurman L, Roy C, Schoemaker RC, Hazekamp A, den Hartigh J, Bender JC, Verpoorte R, Pinquier JL, Cohen AF, van Gerven JM. Effect of intrapulmonary tetrahydrocannabinol administration in humans. J Psychopharmacol 2008; 22: 707–16.

16 Zuurman L, Roy C, Schoemaker R, Amatsaleh A, Guimaeres L, Pinquier J, Cohen A, van Gerven J. Inhibition of THC-induced effects on the central nervous system and heart rate by a novel CB_1 receptor antagonist AVE1625. J Psychopharmacol 2010; 24: 363–71.

17 Klumpers LE, Fridberg M, de Kam ML, Little PB, Jensen NO, Kleinloog HD, Elling CE, van Gerven JM. Peripheral selectivity of the novel cannabinoid receptor antagonist TM38837 in healthy subjects. Br J Clin Pharmacol 2013; 76: 846–57.

18 Beal S, Sheiner LB, Boeckmann A, Bauer RJ. NONMEM User's Guides. (1989–2009), Icon Development Solutions, Ellicott City, MD, USA, 2009. In: Book NONMEM User's Guides. (1989–2009). Ellicott City, MD, USA: Icon Development Solutions, 2009 City; 2013.

19 Holford NH, Sheiner LB. Pharmacokinetic and pharmacodynamic modeling *in vivo*. Crit Rev Biomed Eng 1981; 5: 273–22.

20 Tonstad S, Aubin HJ. Efficacy of a dose range of surinabant, a cannabinoid receptor blocker, for smoking cessation: a randomized controlled clinical trial. J Psychopharmacol 2012; 26: 1003–9.

21 Bowdle TA, Radant AD, Cowley DS, Kharasch ED, Strassman RJ, Roy-Byrne RP. Psychedelic effects of ketamine in healthy volunteers. Relationship to steady-state plasma concentrations. Anesthesiology 1998; 88: 82–8.

22 Groenendaal D, Freijer J, Rosier A, de MD, Nicholls G, Hersey A, Ayrton AD, Danhof M, de Lange EC. Pharmacokinetic/pharmacodynamic modelling of the EEG effects of opioids: the role of complex biophase distribution kinetics. Eur J Pharm Sci 2008; 34: 149–63.

23 Hull CJ, Van Beem HB, McLeod K, Sibbald A, Watson MJ. A pharmacodynamic model for pancuronium. Br J Anaesth 1978; 50: 1113–23.

24 Sheiner LB, Stanski DR, Vozeh S, Miller RD, Ham J. Simultaneous modeling of pharmacokinetics and pharmacodynamics: application to d-tubocurarine. Clin Pharmacol Ther 1979; 25: 358–71.

25 Martinez J, Fabre D, Kanamaluru V. Population pharmacokinetics of rimonabant in obesity. PAGE 2007; 16.